THE ASTROPHYSICAL JOURNAL, 284:98–107, 1984 September 1

THE EVOLUTION OF ASYMPTOTIC GIANT BRANCH STARS IN THE LARGE MAGELLANIC CLOUD

NEILL REID
University of Sussex and Royal Greenwich Observatory

AND

JEREMY MOULD[1]
Palomar Observatory, California Institute of Technology
Received 1983 November 21; accepted 1984 March 9

ABSTRACT

We present a bolometric luminosity function for stars on the asymptotic giant branch (AGB) in a 15 deg^2 area of the Large Magellanic Cloud (LMC). The luminosity function was derived by COSMOS scanning of multiple visual and infrared UK Schmidt plates and is photometrically complete for $V-I > 1.6$. The deficiency of luminous AGB stars which was apparent in earlier spectroscopic studies is seen in this study also. This rules out the notion that the deficiency is due to nuclear processing of carbon-rich envelopes to spectroscopically normal composition. A more likely explanation is that mass loss more severe than is predicted by standard scaling relations sets in on the upper AGB, terminating the evolution of these stars at quite modest luminosities. Significant variations in the AGB luminosity function are seen over the field. These are best understood as a consequence of different star formation histories in different locations in the LMC.

Subject headings: galaxies: Magellanic Clouds — galaxies: stellar content — luminosity function — stars: late-type — stars: mass loss

I. INTRODUCTION

In their final stage of evolution as red giants, intermediate-mass stars exhibit the effects of a number of uniquely interesting astrophysical processes. These include mixing to the stellar photosphere of products of interior nucleosynthesis, mass loss from the stellar surface, and the return to the interstellar medium of processed material. The economics of white dwarf and supernova formation are governed by the extent of mass loss in this phase.

Recent progress in the theory of asymptotic giant branch (AGB) evolution has been reviewed by Iben and Renzini (1983). At this point, it is clear that the theory of double-shell source stars undergoing thermal pulses is qualitatively capable of producing the kinds of stars that are observed. Detailed quantitative comparison of observations and theory are now required to constrain the mass loss parameterization and to test surface composition predictions. A populous stellar system should be the site of this investigation, since AGB evolution occurs on a 10^6 year time scale. The Magellanic Clouds represent the ideal laboratory for the study of AGB evolution.

In this paper we carry out the groundwork for such a study by isolating a sample of Large Magellanic Cloud (LMC) AGB stars. Photometry of a 15 deg^2 field north of the Bar is performed from UK Schmidt plates (§ II). In § III a spectroscopically unbiased AGB luminosity function is constructed for stars between -4 and -7 in M_{bol}. Finally, in § IV we compare the results with simple models for the star formation history of the LMC.

II. THE SURVEY

Previous large-scale searches for late-type stars in the Magellanic Clouds have either been based on objective prism techniques—using the Uppsala Southern Schmidt (Westerland, Olander, and Hedin 1981) and the University of Michigan Curtis Schmidt (Sanduleak and Philip 1977) telescopes—or been limited to LMC clusters (Mould and Aaronson 1982; Lloyd Evans 1980). The latter surveys are restricted in area and, as a result of the spectroscopic criteria used, all of the former surveys are limited to carbon stars and very late type M stars. Of the objective prism surveys, only the 4 m prism survey (Blanco, McCarthy, and Blanco 1980, hereafter BMB) goes fainter than $I \sim 14$, and it is restricted to 0.36 deg^2 in the LMC and 0.24 deg^2 in the SMC. With the advent of fast, accurate, automated scanning microdensitometers and the availability of high-quality I-band direct plates from the UK Schmidt telescope, similar surveys can now carried out using purely photometric criteria. While this method sacrifices carbon star discrimination, our sample can be extended to include all stars on the AGB [corresponding to a cutoff of $(V-I) > 1.6$].

Our survey covers 15.62 deg^2 within the UK Schmidt field centered on R.A. = 5^h20^m, decl. = $-66°48'$. The area sampled is $\sim 4.°35$ (east-west) by $\sim 3.°82$, with the southernmost point 1.°0 north of 30 Doradus. As is further described below, with the Schmidt plate scale of 67.″14 per millimeter image crowding is a major limitation, and several regions of particularly high star density have been excluded. In addition we have removed the areas around the brightest stars, where halation rings and diffraction spikes are dissociated into numerous spurious images by microdensitometers.

a) Photometry

Five I (IVN + RG 715) and three V (IIaD + GG 495) plates were used in this investigation. All were measured on the COSMOS facility at the Royal Observatory of Edinburgh, providing parameterized data (size, shape, position, and magnitude) to a limiting magnitude of $I \sim 17$ and $V \sim 18$—

[1] Visiting Astronomer, Cerro Tololo Inter-American Observatory, which is operated by AURA, Inc., under contract to the National Science Foundation.

although the data are incomplete for $V > \sim 17$ and $I > \sim 16$. Magnitude calibration is achieved by polynomial fitting of the relation between instrumental and photoelectric magnitude (Reid and Gilmore 1982). This calibration is largely based on V and I CCD frames obtained at the prime focus of the 4 m at Cerro Tololo Inter-American Observatory (CTIO) in six 14 arcmin^2 fields. These were reduced and standardized in the manner described by Mould and Aaronson (1982). Primary standards used in this calibration were taken from the E2 and E3 regions (Graham 1981), NGC 300 (Graham 1982), RU 149 ($V-I = -0.16$; A. U. Landolt, private communication), and G161-33/34 ($V-I = 2.33, 2.87$; Rodgers and Eggen 1974). The latter two stars were transformed from the Eggen-Kron system following Bessell (1979). The zero point and color term of the CCD calibration are formally determined to 0.01 mag. The secondary standards used in turn to calibrate the photographic data also spanned a wide color range (0.5–2.6 in $V-I$).

In addition to these stars, which cover the range $14 < V < 17.5$ and $12 < I < 15.5$, we have used V photometry by Butler (1972) and Walker (1974) and photoelectric I photometry by O. J. Eggen (private communication). A few additional bright I standards were obtained by applying the mean $(B-V)$-$(V-I)$ relation to standards with $0.2 < (B-V) < 1.0$. This relation is reddening independent provided that the LMC reddening law is similar to that in the Galaxy, as observations suggest (Koornneef 1981), and provided that $E(B-V) < 0.25$. The color excess is less than 0.04 for all the standards used here. All of the I-band photometry has been transformed onto the Kron-Cousins system (which has the same effective wavelength as the Schmidt I passband—Blair and Gilmore 1982), while a color term [slope 0.08 in $(V-I)$] is included in the V photographic calibration. The latter is derived from photoelectric standards in the south galactic field (Reid and Gilmore 1982) and well represents the data to at least $(V-I) = 2.6$.

Table 1A gives the rms residuals associated with each individual calibration. These indicate uncertainties of 0.11 in V and 0.08 in I for stars on all three V and all five I plates. The internal consistency (plate to plate) can be judged by considering the mean rms error of an individual measurement which for stars with $V < 18$ and on at least two V plates is ~ 0.12 and is ~ 0.11 for stars $I < 15.5$ and on at least three plates (Reid 1983).

The sky background determination represents a possible source of systematic errors. The effective COSMOS spot FWHM (excluding halo) for our measurements was 25 μm (Hewett 1982) with measuring increments (pixel sizes) of 8 μm and 16 μm. Both plates measured at the latter increment showed systematic positional effects in magnitude when compared with the 8 μm measures. These were correlated with the number density of images and were also apparent as variations in the "sky" determinations. Hence they are most probably due to the larger pixel size smearing faint stars and the wings of brighter images in "sky" pixels. As a check on the performance of COSMOS at 8 μm pixel size, two plates (V1133 and I4693) were also measured on the APM facility at Cambridge, which has a significantly smaller scanning spot (Gaussian core of less than 8 μm). There were no systematic differences of more than 0.07 mag between the measures, and the random errors machine to machine are identical with those found in repeated COSMOS measures. We have applied small (<0.1 mag) zero-point corrections to the affected regions in the two 16 μm measures. Overall, it is likely that systematics limit our photometric accuracy to ~ 0.1 in I and ~ 0.15 in $(V-I)$.

b) Image Crowding and Completeness

The COSMOS image analysis algorithm works on the basis of identifying and linking contiguous pixels with densities more than a given threshold above sky level. Thus close pairs of stars merge into single images in the eye of the machine. Even though regions of particularly high star density are excluded from our sample *a priori*, "merged" images constitute a significant fraction of the data. However, the bulk of these images are easily recognized through their having high ellipticity. Table 1B shows the ellipticity (b/a) distribution for a complete sample of single and merged images (classified by eye) within a typical 3 × 3 cm area. The data shown are from the COSMOS scans of I4693 and V974, but the distributions are representative of I and V plates respectively. (All three V plates show a broader ellipticity distribution.) As expected, merged images have, on average, smaller axial ratios. Working from these distributions, together with data from the other scans, we have accepted as single stars images with $b/a > 0.65$ on at least three I plates and one or more V plates. This reduces the total sample by 15.6%, with a slightly higher fraction of bright stars excluded (cf. Table 1B). Demanding good images on at least two V plates cuts the numbers by a further 10%. However, the fractional reduction (based on the V plate images) is essentially constant with I magnitude, so the shape of the (logarithmic) AGB luminosity function is little affected, as is discussed in § III.

We have used the CCD I images to check on the magnitude limit for completeness. For the present survey for AGB stars, $I \sim 14.5$ is the required limiting magnitude, and all stars with $I < 15$ on the CCD frames are present on the COSMOS scans (15% fail the ellipticity criteria outlined above). Hence from the results of Table 1B, we expect $\sim 6\%$ of our final sample to be "merged" images. Overall, image crowding problems mean that the absolute luminosity function is uncertain by 20%–30%. However, since there is no dramatic variation in image

TABLE 1A

COSMOS Scanning Log

Plate	Epoch	Grade	Exposure (minutes)	n (standards)	σ Increment	Microns
V974	1974 Oct 23	A–	40	50	0.16	8
V1133	1975 Jan 14	A	40	51	0.22	8
V1154	1975 Jan 17	B	40	50	0.18	8
I3719	1977 Nov 3	A	90	67	0.15	16
I4636	1978 Nov 21	A	90	63	0.20	16
I4693	1978 Dec 7	A	90	66	0.18	8
I5457	1979 Nov 13	A–	90	65	0.15	8

TABLE 1B

ELLIPTICITY DISTRIBUTIONS FOR SINGLE AND MERGED IMAGES WITHIN A 3 × 3 CENTIMETER AREA NEAR NGC 2040

	$11 < I < 13$				$13 < I < 15$			
	I4693		V974		I4693		V974	
b/a	Single	Merged	Single	Merged	Single	Merged	Single	Merged
0.25–0.30.....	...	1	...	...	1	1	...	3
0.30–0.35.....	...	3	...	3	...	5	2	3
0.35–0.40.....	1	4	2	6	...	15	10	5
0.40–0.45.....	...	11	7	12	2	18	30	16
0.45–0.50.....	1	14	8	20	1	17	25	27
0.50–0.55.....	3	13	19	16	2	27	35	30
0.55–0.60.....	2	19	13	25	5	22	20	24
0.60–0.65.....	1	10	16	14	10	29	43	30
0.65–0.70.....	1	21	21	10	18	18	51	24
0.70–0.75.....	12	9	22	12	34	11	59	14
0.75–0.80.....	17	7	48	5	57	4	86	13
0.80–0.85.....	37	1	37	1	140	4	115	2
0.85–0.90	92	...	55	3	291	1	221	3
0.90–0.95.....	146	1	78	2	410	4	159	2
0.95–0.100.....	90	...	42	...	173	2	87	2

crowding over the range $10 < I < 15$, the relative luminosity function is accurate to better than 10%.

One specific problem must be considered, however. Since the limiting magnitude in V is ~ 18.5, even with this bright limit in I the reddest AGB stars are measured by COSMOS only on the I plates. However, objects merged with other images obviously have distorted (x, y) centroids and fail to match in the plate pairing process, adding to the apparently very red, "unpaired" stars. For this reason, all 452 unpaired images with $I < 15$ were checked by eye. Only six prove to be genuine very red stars. Of the remainder, 126 are close pairs of stars merged in I (these all fail the ellipticity criterion described above): 280 are stellar pairs (or multiples) merged in V; 44 lie within LMC clusters; 45 are lost in nebulosity on the V plate; four are merged with galaxies and five with bright star diffraction spikes. Estimating magnitudes from visual inspection, it is unlikely that more than 100 of these have AGB star colors. In fact, only the I plate merges are relatively red stars, since stars merged in V but not in I tend to be brighter (larger) on the former plates, i.e., blue stars.

All six very red stars are just detectable by eye on the deeper V plates, although absent from the COSMOS measures, implying V magnitudes of ~ 19.5 and $(V-I) \sim 4.5$–5. Hence, only 14 stars within our 16 deg^2 area have $I < 15$ and $(V-I) > 4.5$. The implications of this result are further discussed below.

Finally, we can use the carbon star survey by Westerlund, Olander, and Hedin (1981) for an empirical test of our completeness. Of the 46 stars within our area, seven (15%) are merged in V or I, while two [no. 67 $(V-I) = 1.42$) and no. 106 $(V-I) = 1.40$] are bluer than our AGB limit. Photoelectric photometry by Westerlund *et al.* shows that no. 67 has $(R-I)_J = 0.87$; hence the results of this comparison are generally consistent with our predictions.

III. THE ASYMPTOTIC GIANT LUMINOSITY FUNCTION

Table 2 presents the $[I, (V-I)]$ color-magnitude diagram for the regions surveyed in the LMC. Our star counts are binned in 0.25 mag intervals in I and $(V-I)$ over the range $8 < I < 15$ and $-0.5 < (V-I) < 5.5$. The tabulated data also include the contribution from foreground galactic stars. Galaxy star count models (G. Gilmore, private communication) show that the latter are almost exclusively disk red dwarfs with absolute magnitudes $M(v) > 7.5$ $[M(I) > 6.0]$. We have calculated their contribution to Table 2 by transforming the disk luminosity function tabulated by Gilmore and Reid (1983) to $M(I)$ and modeling the density distribution perpendicular to the plane by a 300 parsec scale height exponential disk. Table 3 lists the total numbers of foreground dwarfs expected in our survey. Allowing for merged images, these represent a less than 10% contamination at all magnitudes. A spectroscopic survey of AGB candidates confirms that contamination may be as low as 5% (Mould and Reid 1984).

To form the AGB luminosity function from the color-magnitude diagram of Table 2, we exclude all stars with $V-I < 1.6$. This is the color of the M92 giant branch tip (Mould, Kristian, and Da Costa 1983), reddened by $E(B-V) = 0.1$ $[E(V-I) = 0.125]$. That value of the reddening is a mean for the field based upon the photometric catalog of Rousseau *et al.* (1978) and the intrinsic colors given by Fitzgerald (1969). Hence we expect to retain in our luminosity function all AGB stars brighter than the core helium flash, even if they are as metal poor as M92. On the other hand, first giant branch stars will begin to appear (and dominate the sample) for $M_{bol} > -3.6$. Bolometric magnitudes were derived using the relation

$$M(\text{bol}) = I + 0.906 - 0.246\,(V-I-0.125) - 18.7$$

calibrated by globular cluster giants to $(V-I) = 2$ (Mould, Kristian, and Da Costa 1983). The last term is the adopted apparent distance modulus of the LMC. This is the mean of several determinations (see Mould, Da Costa, and Crawford 1984) which are not in very good agreement. It should be considered uncertain by 0.3 mag.

We noted above that the shape of the AGB luminosity function was not sensitive to our image quality criterion. Table 3 gives the number of AGB stars deduced by (*a*) limiting the sample to stars with at least two good V measurements or (*b*) including stars with reliable V magnitudes from one or more plates. As Figure 1 shows, while the scale of the function

TABLE 2

COLOR-MAGNITUDE DIAGRAM

	$V-I$																								
I	−0.63	−0.38	−0.13	0.13	0.38	0.63	0.88	1.13	1.38	1.63	1.88	2.13	2.38	2.63	2.88	3.13	3.38	3.63	3.88	4.13	4.38	4.63	4.88	5.13	5.38
8.13		1		1	1	1	3	4	4	5	3				1										
8.38							3	1	4	8	3	1	1												
8.63					1	2	1	4	6	5	3	2						1							
8.88		1			2	1	1	4	8	3			1	1	1		1								
9.13	1			2		1	2	4	9	3			2												
9.38			1		1	3	7	7	9	3							1								
9.63				1		2	10	14	7	6	1	1	2		2		1								
9.88	2	2		2		13	15	18	9	9		2			2										
10.13				1	1	7	8	12	10	7	2	1	1												
10.38	1		1		1	12	20	21	12	5	5	6	4	2	1							1			
10.63	2		1	2	5	14	27	23	15	4	2	2	1												
10.88	1	1	2	3	4	19	32	27	13	5	7	3	1			1									
11.13				1	6	26	36	32	14	4	13	3		1		2	1								
11.38		1	1	5	10	37	63	38	17	11	9	3		1											
11.63		2	3	8	9	62	79	40	13	16	8	3	1	1	1										
11.88	1		3	12	11	65	92	42	12	13	8	2	2			1	1								
12.13			3	3	21	73	104	34	21	20	12	8		1	3	1									
12.38	3		6	12	26	99	159	60	33	16	8	12	6	1	1		1			1					
12.63			3	7	31	126	175	72	33	38	10	11	13	6	1	1	5	1	1	2			1		1
12.88	1	2	5	14	36	152	166	79	48	30	19	15	13	8	10	9	2	2	1				1		
13.13	6	4	8	30	42	142	200	105	63	44	31	28	28	20	13	8	1	2	1		1				1
13.38			11	49	42	152	230	126	83	54	41	47	59	37	32	17	8	5	4	1		1			
13.63	3	3	14	46	74	194	266	139	93	77	71	97	90	98	48	47	32	13	7	3					
13.88	1	8	30	54	70	206	341	165	131	104	95	149	141	119	93	73	46	15	9	7	1	1			
14.13	1	10	35	68	96	249	369	257	172	145	141	170	156	83	69	39	11	14	5	5		1			
14.38	3	13	53	82	106	255	456	306	293	275	286	197	89	55	27	18	9	10	1						
14.63	4	11	62	93	136	305	488	388	360	689	616	286	93	26	20	8	3	4	2	2					
14.88	6	26	88	116	136	335	557	573	697	1033	737	274	65	31	13	5	7				1				

TABLE 3

BOLOMETRIC LUMINOSITY FUNCTIONS

		AGB STARS[a]		QUADRANTS			
M_{bol}	FOREGROUND	(*a*)	(*b*)	SE	NE	SW	NW
−7.45	2.25	13.75	14.75	6.44	1.44	2.44	4.44
−7.2	2.20	19.8	19.8	9.45	3.45	4.45	2.45
−6.95	2.40	21.6	22.6	12.40	2.40	3.4	4.4
−6.7	2.80	23.2	26.2	14.30	–	8.3	4.3
−6.45	3.70	26.3	29.3	16.08	1.08	6.07	6.07
−6.2	4.90	43.1	46.1	24.77	3.78	8.77	8.77
−5.95	6.7	54.3	60.3	19.33	5.33	20.33	15.32
−5.7	9.3	80.7	92.7	32.67	14.68	27.67	17.67
−5.45	13	125	143	48.75	16.75	48.75	28.75
−5.2	19	240	266	86.25	45.25	79.25	53.25
−4.95	28	481	531	159	95	158	118
−4.7	41	608	662	187.75	136.75	199.75	135.75
−4.45	60	559	609	182	103	202	120
−4.2	88	536	593	178	104	196	114
−3.95	73	407	447	139.75	68.25	152.50	86.50
−3.7							

[a] Number of AGB stars deduced by (*a*) limiting the sample to stars with at least two good V measurements or (*b*) including stars with reliable V magnitudes from one or more plates.

changes, the general characteristics and overall shape are invariant.

These data are for a limiting magnitude of $I = 14.5$. As Figure 1 shows, lowering the apparent magnitude limit to $I = 15$ only affects the last bin of the bolometric luminosity function, adding stars at the tip of the LMC first red giant branch. The brighter limit is obviously more appropriate for the present study.

Figure 2 shows the spatial distribution of the $I = 14.5$ limited sample. With the caveats that even in our large sample we are dealing with small numbers of bright stars and that several circular areas have been excluded to avoid the halos of *very* bright stars, it is clear that there is a trend in declination in the relative numbers of bright (Fig. 2*b*) and faint (Fig. 2*a*) stars. To quantify this trend, Table 3 presents separate luminosity functions for stars in quandrants of approximately equal areas. We shall argue in § IV that a difference in the star formation history of these regions is responsible for this effect.

IV. A THEORETICAL AGB LUMINOSITY FUNCTION

According to AGB evolutionary theory by Iben and Truran (1978) and Renzini and Voli (1981), the luminosity of the tip of the AGB is a monotonic increasing function of stellar mass. This prediction is verified in the survey and photometry by Aaronson and Mould (1982), where peak luminosities in clusters are seen to correlate with the age ranking by Searle, Wilkinson, and Bagnuolo (1980). This means that, at any point on the AGB luminosity function of Figure 1, contributions are made only by stars younger than a certain age.

This notion can be developed into a model of the AGB luminosity function, if we adopt a relation between peak luminosity, $M_{bol,f}$ and age, such as that calculated by Mould and Aaronson (1982) with certain assumptions (Reimers 1975) about the mass loss rate for red giants. Since the AGB luminosity function for a single system of age t_9 (Gyr) is flat, as a result of the core mass–luminosity relation (Renzini 1977), the

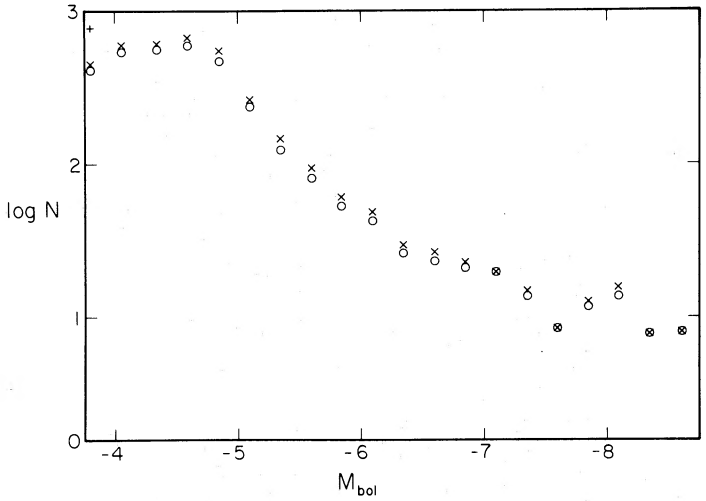

FIG. 1.—The AGB luminosity function from Table 3. Open circles are data from AGB stars column (*a*) and crosses are data from column (*b*). The plus sign indicates the effect of dropping the limiting magnitude in I to 15. Only the faintest bin is affected.

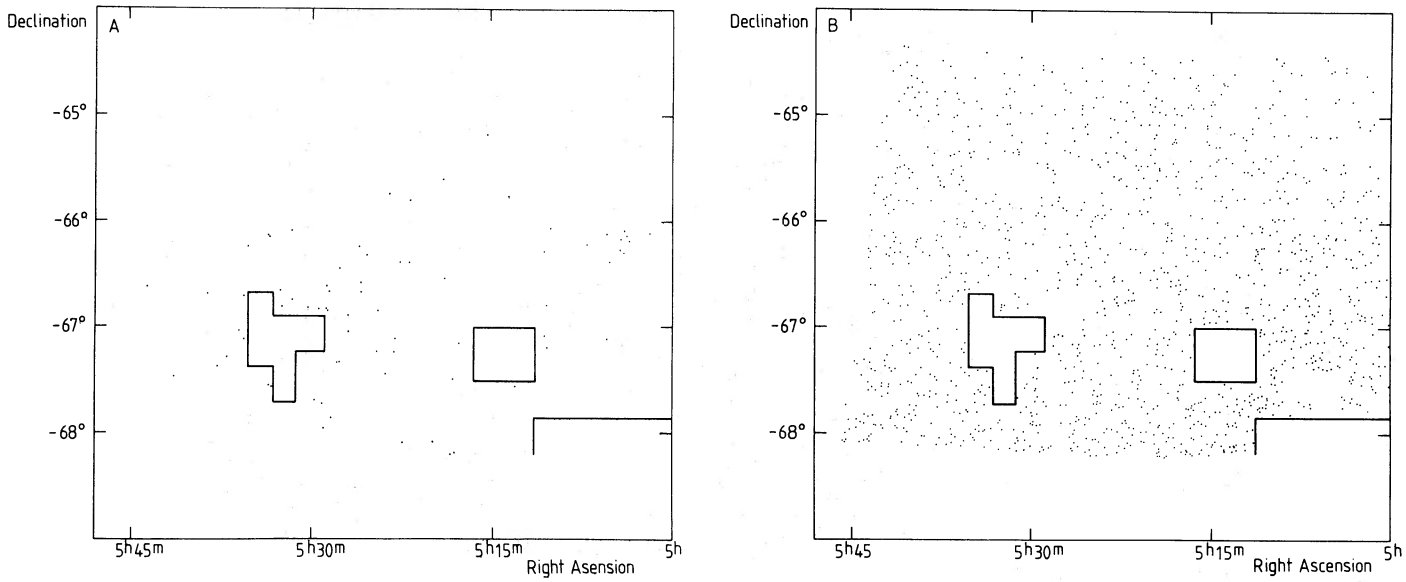

FIG. 2.—The distribution on the sky of stars counted in Table 3 column (*a*). Bright AGB stars ($-7.5 < M_{bol} < -6.5$) are plotted in Fig. 2*a*, and faint AGB stars ($-4.5 < M_{bol} < -4$) in Fig. 2*b*. The areas marked because of crowding are explicitly shown.

only other function required to calculate a model is the star function history of the field, for which we assume:

$$\text{SFR} = \exp\left[-(t - t_9)/\alpha\right] \quad (t_9 < t)$$
$$= 0 \quad (t_9 > t)\,,$$

where t is the elapsed time in Gyr, since star formation began and α has the character of a time constant. The quantity SFR is the star formation rate in Gyr^{-1}.

In its simplest form, the model is calculated in the following manner. For a given luminosity M_{bol}, the AGB lifetime for a star to rise from $M'_{bol} = -4$ is

$$dt = 1.3 \times 10^{-3}(M_{bol} + 4)\ \text{Gyr}$$

according to Renzini (1977, eq. [6.18]). In this time, stars within a mass increment dm have evolved off the main sequence (Renzini 1977, eq. [2.5]). The number of these stars is given by $m^{-2.35}$ SFR (t), where we have assumed a Salpeter initial mass function (IMF). These stars are distributed uniformly from -4 to M_{bol} in the luminosity function, and the process is repeated to complete an integration from $t_0 < t_9 < t$, where t_0 is the main-sequence lifetime of the most massive star. The calculation will be accurate provided $dt \ll t_0$. The standard model has $t_0 = 0.03$ Gyr and $t = 16$ Gyr.

Before comparing these simple models with the observations, we add two extra features. First, we treat the post–helium-flash dip, in which a thermal pulsing AGB star briefly fades by 0.5 mag following each shell flash (Iben 1981), by assigning 10% of the AGB stars to the 0.25 mag bin below the calculated luminosity and 10% to the one below that. The effect is slight, and the level of approximation, appropriate. Second, we calculate the effect of stars more massive than considered in the simple model in their first red giant branch (RGB) and AGB stages. These stars have $M > 5\ M_\odot$ in the standard model and leave the main sequence before t_0. This calculation was based upon the lifetime of models by Becker, Iben, and Tuggle (1977) and Becker and Iben (1979) in the region $\log T_e < 3.65$. The cutoff effective temperature was hotter than that applied to the observations in order to overestimate the massive star contribution and compensate for mixing length uncertainties in stellar models. The mass spacing of the models necessarily makes the treatment coarser still.

Figure 3 is a comparison of the minimum assumption ("standard") model for the entire LMC field with data over the full range of the upper AGB, i.e., over the interval -4 to -7 in M_{bol}. Below this luminosity range, we expect large numbers of low mass RGB stars. At $M_{bol} = -7$, an AGB star has a core mass approaching the Chandrasekhar limit. The standard model has $t = 16$ Gyr and $\alpha \to \infty$ (i.e., constant star formation). It was normalized to the data at the second 0.25 mag bin. Two conclusions stand out from this comparison. First, there is a marked deficiency of stars in the interval $-6.5 < M_{bol} < -5$, and second the massive star contribution is apparently relatively small. Although the standard model predicts that this contribution is less than 10% at all magnitudes, the absence of an abrupt edge in the luminosity function (Fig. 1) at the AGB tip (-7.2 mag) suggests that the model may underestimate this contribution. This could be due either to an unsatisfactory estimate of the lifetimes of these stars or to a recent burst of star formation in the last 10^8 years.

A deficiency of luminous AGB stars like that seen in Figure 3 was first brought to light as a result of the infrared grism surveys for late type M and C stars by BMB. Iben (1981) pointed to this deficiency as one facet of the carbon star "mystery," asking "where have all the high mass ones gone?" Figure 4 offers a direct comparison of our results with those of BMB for their "bar west" field. This field of theirs is the most thoroughly studied, in that Frogel and Blanco (quoted by Frogel and Richer 1983, hereafter FR) have reexamined the grism plate to include early M stars in addition to the late-types selected by BMB, and FR have conducted a single-channel photometric survey of 64% of the area of the field to search for additional objects missed spectroscopically. Bolometric corrections were applied to the BMB magnitudes (see, for example, Cohen *et al.* 1982) to construct the histogram given in Figure 4. We also added 1.5 times the number of stars

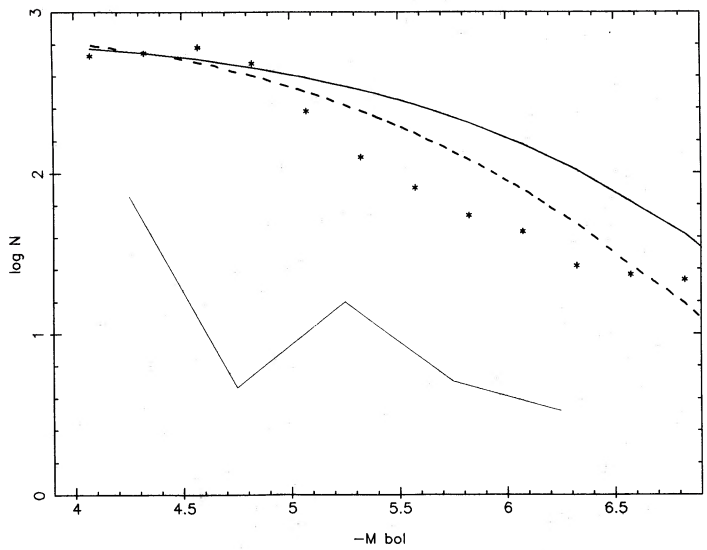

FIG. 3.—Predicted bolometric luminosity function (*solid curve*) for the standard model with age 16 Gyr and constant SFR. The dashed curve has an IMF slope of 3.35. The models are normalized to the observed star counts (*asterisks*) in the −4.2 to 4.45 interval. The lower (*light line*) curve is an approximate treatment of the contribution from RGB and AGB stars more massive than 5 $M_{\odot}$, which should be added to the standard model.

found by FR to the distribution, where they are identified separately from the C and M stars of BMB. The comparison between the two luminosity functions (*histogram and solid circles*) in Figure 4 shows quite reasonable correspondence. But this is partly fortuitous, since the early M stars of Frogel and Blanco are not included here and we have already demonstrated that the luminosity function is position dependent in our large area. To zeroth order, however, both samples do register a similar deficiency of luminous stars relative to a constant SFR model. The solid curve in Figure 4 represents such a constant SFR model with age (t) of 7 Gyr (cf. Fig. 3). The discrepancy is gross, a factor of 3 at $M_{\rm bol} = -6$. The exact factor is dependent on the assumed slope of the IMF. Figure 3 shows that, if the IMF slope is changed from −2.35 to −3.35, a slightly better fit is obtained, but the discrepancy remains. However, there is no evidence to support such a steep IMF either in the solar neighborhood (where the slope in the relevant 1 $M_{\odot} < M < 5\ M_{\odot}$ range is slightly shallower than the Salpeter value, Tinsley 1980) or in the LMC (Dennefeld and Tammann 1980).

Figure 4 also demonstrates one method of reconciling theory and observation. That is to postulate that the SFR in the LMC has fallen dramatically from an epoch 7 Gyr ago to the present time. The corresponding model shown in Figure 4 has $t = 7$ and $\alpha = 2$ Gyr, which means that star formation began suddenly in the LMC 7 Gyr ago, but declined exponentially to a current rate just 3% of the initial rate. Evidence has accumulated lately (e.g., Butcher 1977; Styker, Butcher, and Jewell 1981; Hardy *et al.* 1983) in favor of the view that the initial burst of star formation in the LMC did occur as recently as this

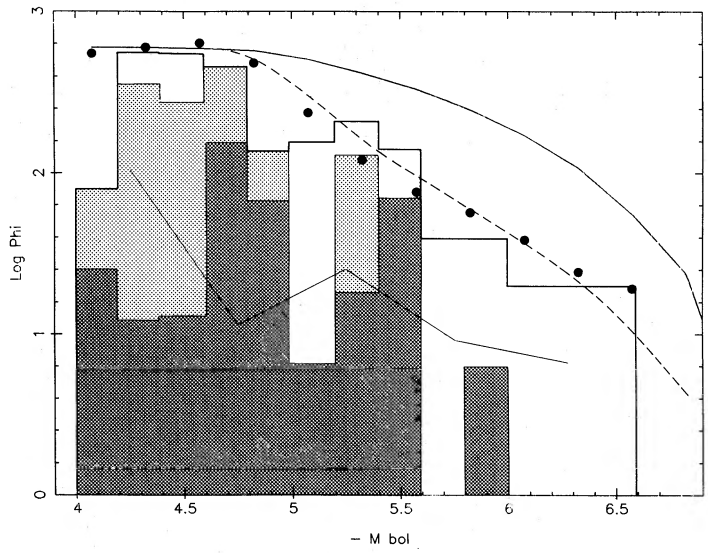

FIG. 4.—A luminosity function constructed from the spectroscopic survey by BMB and infrared survey by FR and scaled up by a factor of 20 for comparison with the present results (*filled circles*). The solid curve is a constant SFR model with $t = 7$, $\alpha = 2$ Gyr. The shading of this histogram shows how this luminosity function is partitioned (on a linear, not logarithmic, scale) into C stars (*dark*), M stars (*light*) from BMB, and photometric AGB stars (*unshaded*) from FR.

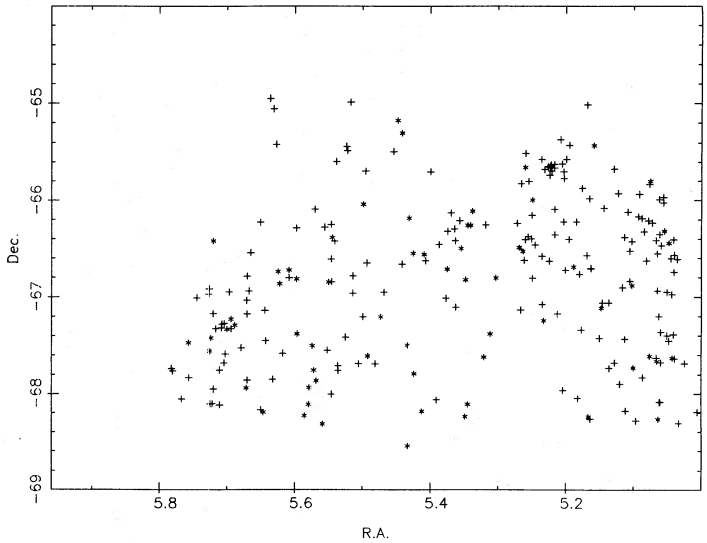

FIG. 5.—The distribution of Cepheid variables over the field from Payne-Gaposchkin (1971). Crosses have periods greater than 5 days, asterisks less than 5 days.

(or perhaps more recently), but the idea of a declining SFR may be less acceptable. In particular we note the following points.

1. A more extreme version of the idea (*no* recent star formation) was first proposed by Iben (1981) and rejected by Becker (1982) on the basis of a Cepheid count. Becker found 10 Cepheids in the BMB Bar-West field, which scales to 200 Cepheids in the present field with the normalization used to construct Figure 4. Approximately 240 Cepheids are listed in the present field by Payne-Gaposchkin (1971), so it is clear that *some* star formation has been going on there in the last few hundred million years. The distribution of Cepheids in the field is shown in Figure 5, separated by different symbols for periods greater than or less than 5 days. When compared with Figure 2, both distributions resemble that of the more luminous ($M_{\rm bol} < -5.5$) AGB stars. This is to be expected, since the Cepheids have an age of the order of 10^8 years and would evolve all the way to the AGB limit in their own double-shell source phase. At the same time, it would be impossible to deny from Cepheid data alone the possibility that the SFR in this field might be much lower than in the past. According to Becker, Iben, and Tuggle (1977), prediction of total Cepheid counts is far too composition dependent to constrain our models accurately.

2. A star formation history with such a dramatic decline would predict a sharp break at the AGB limit ($M_{\rm bol} < -7$). This would be at least an order of magnitude based on the massive star contribution estimate in Figure 3. No such break is seen in Figure 1. This argument is in the same vein as the previous one, but the uncertainties relate more to red supergiant evolution (see Maeder 1981).

3. The star formation history of the solar neighborhood deduced from dwarf stars by Twarog (1980) is constrained by $\langle \mathrm{SFR} \rangle / \mathrm{SFR}_0 < 2.5$. This compares with $\langle \mathrm{SFR} \rangle / \mathrm{SFR}_0 = 9.2$ for the exponentially declining model in Figure 3. Main-sequence color-magnitude diagrams for the LMC and the solar neighborhood (see Butcher 1977), however, suggest that the LMC should have the lower ratio of the two.

None of these arguments are watertight. But they do suggest that, although it would be possible to contrive a function SFR(t) to fit the AGB luminosity function, a peculiar star formation history is probably not the whole solution to the problem. In passing, we note (Fig. 6) that the two discrete epochs of star formation discussed by Frogel and Blanco (1983), with an efficiency ratio 10:1, do not give a good fit to the data. On the other hand, a *recent* burst of star formation in the LMC would counter some of the objections to the monotonic declining SFR model discussed above.

A second class of solutions to the problem of the missing luminous AGB stars arises from the current state of uncertainty in the mass loss rates for red giants. The peak luminosity attained on the AGB by stars of a given initial mass is critically dependent on the mass loss law. Renzini (1977) and Mould and Aaronson (1982) have employed the Reimers's (1975) expression for the mass loss rate and used the observation that galactic globular cluster AGBs of known age terminate at approximately $M_{\rm bol} = -3.6$ to set the proportionality constant in this expression. It is then straightforward to predict $M_{{\rm bol},f}(t_9)$, which is employed in the current models. Hodge (1983) has pointed out, however, that ages determined from this prediction are systematically larger than those determined from the (albeit sparse) data on main-sequence turnoffs for Magellanic Cloud clusters. In time we can expect better data on Cloud cluster turnoffs from CCD photometry with the large telescopes of the southern hemisphere. But as an exploratory measure we can use Hodge's collation to create an empirical $M_{{\rm bol},f}(t_9)$ relation by drawing a lower envelope to the data plotted in his Figure 5. To support such a relation, Reimers's law would need to be modified in the sense of requiring still higher mass loss rates at higher luminosities. We defer discussion of the ramifications of this (and other possibilities), pending more complete data on Magellanic Cloud globular clusters. The point to be made in the present context is that introduction of this empirical $M_{{\rm bol},f}(t_9)$ relation has the right kind of effect on the model ($t = 16$, $\alpha \rightarrow \infty$), as is shown in Figure 6.

On the other hand, it is clear that modification of the mass loss law cannot completely explain the discrepancy between theory and observation seen in Figure 3. Earlier we noted clear differences among the luminosity functions in the separate quadrants. Figure 7 shows that the luminosity function for the NE quadrant falls systematically further and further below that for the SE quadrant for $M_{\rm bol} < -5$, while the NW and

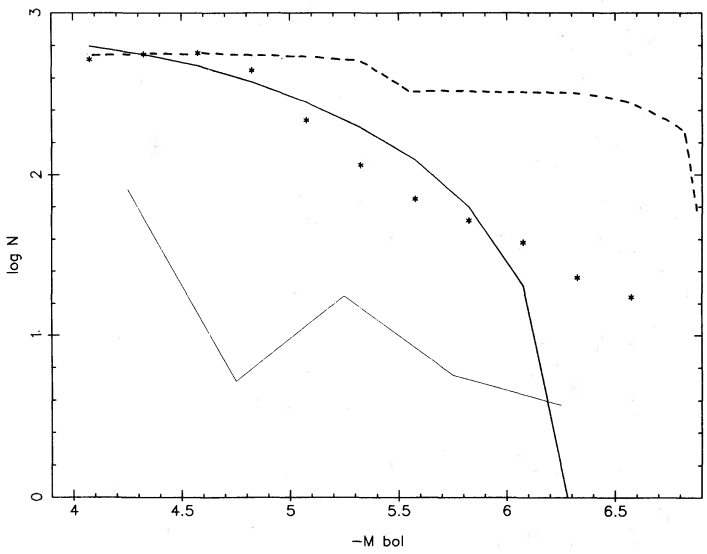

FIG. 6.—The observed luminosity function (*asterisks*) compared with two nonstandard models. The solid curve results from a modified relation between AGB tip luminosity $M_{\text{bol}, f}$ and age (see text). The dashed curve has a modified SFR, incorporating two discrete epochs of star formation.

SW functions are broadly similar in slope and lie in between. All the individual functions remain in disagreement with the standard model. Unless we wish to entertain the possibility of position-dependent mass loss, the implication is clear. Over the last 10^9 years, there have been significant variations in the SFR from place to place in the LMC. This interpretation is supported both by the overall distribution of H I (McGee and Milton 1964) and of nebulae (Davies, Elliott, and Meaburn 1976). In particular, the large ring structure outlined by H II regions, discussed by Davies *et al.*, falls almost entirely within the SE quadrant, while Figure 2*a* shows that the bright stars in the NW and SW quadrants clump near the H II region Henize N13. (Note that both the center of the H II ring and the N30 H II complex in the SW quadrant have been excluded.) Finally, the H I contours show a relatively sharp northern edge and extend only slightly into the NE quadrant—indeed the hydrogen content of the northern third of the field lay below the Parkes detection threshold at the time of Kerr's (1971) review. We would expect a higher than average fraction of RGB stars (core helium burning supergiants) in the star-forming regions of the field. Exactly how large a fraction this is remains to be determined. It cannot be 100% since there is other evidence for the existence of luminous ($M_{\text{bol}} = -7$) AGB stars in the LMC (Wood, Bessell, and Fox 1981).

V. CONCLUSIONS

The important properties of the AGB luminosity function determined here are the large sample, the completeness of the study, and the simple, purely photometric selection criteria. These properties of the survey immediately eliminate one of the solutions to Iben's (1981) "carbon star mystery." In the present luminosity function we see a deficiency of luminous ($-6.5 < M_{\text{bol}} < -5$) AGB stars of all spectral types. The deficiency is not just a deficiency of carbon stars and hence is not due to conversion of carbon stars to M stars by envelope burning.

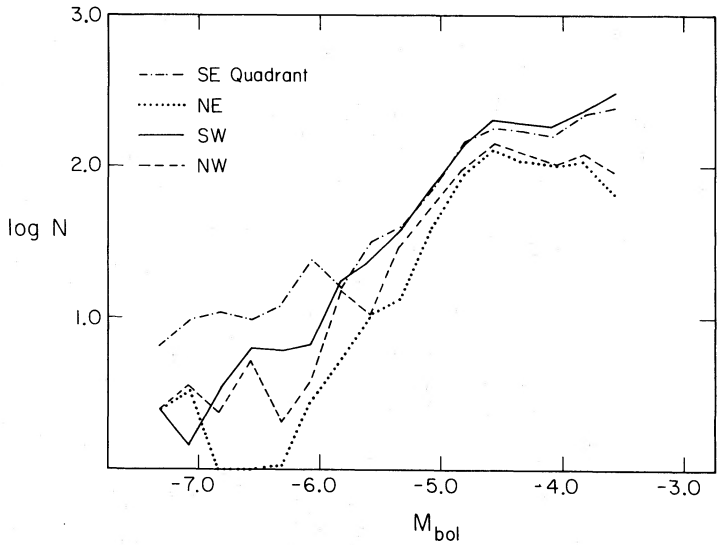

FIG. 7.—Luminosity functions for different quadrants of the field from Table 3

That is not to say that deep envelope burning of carbon to nitrogen may not take place.

In addition, we found very few extremely red stars. Visual examination of unpaired infrared images found only six real stars with $I < 15$. This offers no support for a second hypothesis made by Iben (1981), that the missing AGB stars are concealed by optically thick dust shells. A more severe test of this hypothesis has been performed over a small area by Frogel and Richer (1983).

Perhaps the most important single result from the present survey, however, is the detection of spatial variation in the luminosity function, corresponding to more active and less active star-forming regions. But neither region produces the predicted number of luminous AGB stars, and theory can be most readily reconciled with observation, if we postulate higher mass loss rates for luminous AGB stars (see also Frogel and Richer 1983), which result in their becoming planetary nebulae, *before* the time appointed by the standard theory. This can be investigated directly by correlation of AGB tip luminosities and globular cluster main-sequence turnoffs.

We conclude that the AGB luminosity function is a sensitive probe of the star formation history of the LMC. Once we have determined an empirical relation between stellar age and the extent in luminosity of the AGB, it should be possible to deduce the size and timing of the initial burst of star formation in the LMC, the mean rate of star formation and the presence of subsequent bursts. In addition, we anticipate that a follow-up program of spectroscopy and infrared photometry will better define the characteristics of this sample and allow quantitative estimates of the chemical profile and rate of infusion of AGB products into the interstellar medium.

We would like to thank Olin Eggen for carrying out (R, I) photometry of a number of stars in this field, and Marc Aaronson for assistance with CCD photometry at the CTIO 4 m telescope. This work was partially supported by NSF grant AST-8306139. N. R. acknowledges support from SERC. Part of this work was carried out while N. R. held a Robert Cormack Fellowship at the University of Edinburgh.

REFERENCES

Aaronson, M., and Mould, J. R. 1982, *Ap. J. Suppl.*, **48**, 161.
Becker, S. 1982, *Ap. J.*, **260**, 695.
Becker, S., and Iben, I., 1979, *Ap. J.*, **232**, 831.
Becker, S., Iben, I., and Tuggle, R. S. 1977, *Ap. J.*, **218**, 633.
Bessell, M. S. 1979, *Pub. A.S.P.*, **91**, 589.
Blair, M., and Gilmore, G. 1982, *Pub. A.S.P.*, **94**, 742.
Blanco, V. M., McCarthy, M. F., and Blanco, B. 1980, *Ap. J.*, **242**, 938 (BMB).
Butcher, H. R. 1977, *Ap. J.*, **216**, 372.
Butler, C. J. 1972, *Dunsink Obs. Pub.*, **1**, 6.
Cohen, J. G., Frogel, J. A., Persson, S. E., and Elias, J. 1982, *Ap. J.*, **249**, 481.
Davies, R. D., Elliott, K. H., and Meaburn, J. 1976, *Mem. R. A. S.*, **81**, 89.
Dennefeld, M., and Tammann, G. A. 1980, *Astr. Ap.*, **83**, 275.
Fitzgerald, M. P. 1969, *Pub. A.S.P.*, **81**, 71.
Frogel, J. A., and Blanco, V. M. 1983, preprint.
Frogel, J. A., and Richer, H. B. 1983, preprint.
Gilmore, G., and Reid, N. 1983, *M.N.R.A.S.*, **202**, 1025.
Graham, J. A. 1981, *Pub. A.S.P.*, **93**, 29.
———. 1983, *Pub. A.S.P.*, **94**, 244.
Hardy, E., Buonanno, R., Corsi, C. E., James, K. A., and Schommer, R. A. 1983, preprint.
Hewett, P. C. 1982, Ph.D. thesis, University of Edinburgh.
Hodge, P. W. 1983, *Ap. J.*, **264**, 470.
Iben, I. 1981, *Ap. J.*, **246**, 278.
Iben, I., and Renzini, A. 1983, *Ann. Rev. Astr. Ap.*, **21**, 271.
Iben, I., and Truran, J. W. 1978, *Ap. J.*, **220**, 980.
Kerr, F. J. 1971, in *The Magellanic Clouds*, ed. A. B. Miller (Dordrecht: Reidel), p. 50.
Koornneef, J. 1981, *Astr. Ap.*, **107**, 247.
Lloyd-Evans, T. 1980, *M.N.R.A.S.*, **193**, 87.
Maeder, A. 1981, *Astr. Ap.*, **102**, 401.
McGee, R. X., and Milton, J. A. 1964, in *IAU Symposium 20, The Galaxy and the Magellanic Clouds*, ed. F. J. Kerr and A. W. Rodgers (Canberra: Australian Academy of Sciences), p. 289.
Mould, J. R., and Aaronson, M. 1982, *Ap. J.*, **263**, 629.
Mould, J. R., Da Costa, G. S., and Crawford, M. D. 1984, *Ap. J.*, **280**, 595.
Mould, J. R., Kristian, J., and Da Costa, G. S. 1983, *Ap. J.*, **270**, 471.
Mould, J. R., and Reid, I. N. 1984, in preparation.
Payne-Gaposchkin, C. 1971, *Smithsonian Contr. Ap.*, **13**, 1.
Reid, N. 1983, *Occas. Repts. Roy. Obs. Edinburgh*, No. 10.
Reid, N., and Gilmore, G. 1982, *M.N.R.A.S.*, **201**, 73.
Reimers, D. 1975, *Problems in Stellar Atmospheres and Envelopes*, ed. B. Baschek, W. Kegal, and G. Traving (Berlin: Springer-Verlag), p. 229.
Renzini, A. 1977, *Advanced Stages of Stellar Evolution*, ed. P. Bouvier and A. Maeder (Sauverny: Geneva Observatory).
Renzini, A., and Voli, M. 1981, *Astr. Ap.*, **94**, 175.
Rodgers, A. W., and Eggen, O. J. 1974, *Pub. A.S.P.*, **86**, 742.
Rousseau, J., Martin, N., Prevot, L., Rebeirot, E., Robin, A., and Brunet, J. P. 1978, *Astr. Ap. Suppl.*, **31**, 243.
Sanduleak, N., and Philip, A. G. D. 1977, *Pub. Warney and Swayes Obs.*, **2**, No. 5.
Searle, L., Wilkinson, A., and Bagnuolo, W. 1980, *Ap. J.*, **239**, 803.
Stryker, L. L., Butcher, H., and Jewell, J. 1981, in *IAU Colloquium 68, Astrophysical Parameters for Globular Clusters*, ed. A. G. D. Philip and D. S. Hayes (Schenectady: L. Davis Press), p. 267.
Tinsley, B. M. 1980, *Fundamentals Cosmic Phys.*, **5**, 287.
Twarog, B. 1980, *Ap. J.*, **242**, 242.
Walker, M. 1974, *M.N.R.A.S.*, **169**, 199.
Westerlund, B. E., Olander, N., and Hedin, B. 1981, *Astr. Ap. Suppl.*, **43**, 267.
Wood, P. R., Bessell, M. S., and Fox, M. 1981, *Proc. Astr. Soc. Australia*, **4**, 203.

JEREMY MOULD: Caltech, 105–24, Pasadena, CA 91125

NEILL REID: Royal Greenwich Observatory, Herstmonceux Castle, Hailsham, East Sussex BN27 IRP, England, UK